

Electron localization and entanglement in a two-electron quantum dot

Constantine Yannouleas and Uzi Landman

School of Physics, Georgia Institute of Technology, Atlanta, Georgia 30332-0430

(Dated: 25 January 2005)

Calculations for two electrons in an elliptic quantum dot, using symmetry breaking at the unrestricted Hartree-Fock level and subsequent restoration of the broken parity via projection techniques, show that the electrons can localize and form a molecular dimer, described by a Heitler-London-type wave function. The calculated singlet-triplet splitting (J) as a function of the magnetic field (B) agrees with cotunneling measurements. Knowledge of the dot shape and of $J(B)$ allows determination of the degree of entanglement in the ground state of the dot, which is of interest for the implementation of quantum logic gates. The theoretical value agrees with the experimental estimates.

PACS numbers: 73.21.La, 03.67.Mn

Electron localization leading to formation of molecular-like structures [so-called Wigner molecules (WMs)] within a *single circular* two-dimensional (2D) quantum dot (QD) at zero magnetic field (B) has been theoretically predicted to occur [1, 2], as the strength of the interaction relative to the zero-point energy increases. Of particular interest is a two-electron ($2e$) WM, in light of the proposal [3] for the implementation of a solid-state quantum logic gate that employs two coupled one-electron QDs (double dot).

In currently fabricated circular QDs the strength of the effective Coulomb repulsion is significantly reduced (compared to the value used in Refs. [1, 2], appropriate for bulk GaAs) due to screening from the electrostatic gates and the influence of the finite height of the dot [4, 5]. However, changing the shape of the QD (from a circular shape to an elliptical one, and ultimately to a quasi-linear one) will reduce the zero-point energy, thus enhancing the relative importance of the Coulomb repulsion; this assists in bringing the QD into the strongly correlated regime resulting in electron localization. Here we show that this theoretical prediction [6] has indeed been recently observed experimentally for two electrons in an elliptic lateral QD [7]. We present microscopic calculations for two electrons in an elliptic QD specified by the parameters of the experimental device [7]. These calculations show formation of an electron molecular dimer and yield good agreement with the measured $J(B)$ curve (the singlet-triplet splitting) when the value of the Coulomb repulsion is weakened (by 40%).

Of special interest for quantum computing is the degree of entanglement exhibited by the two-electron molecule in its singlet state [3]. A measure of entanglement, introduced in Ref. [8], is known as the concurrence. To date, however, applications [8, 9] of this measure have been restricted to the specific singlet state associated with the *bonding* and *antibonding* orbitals of a *2e double dot* with weak interdot-tunneling coupling. We show that our *wave-function-based* method enables calculation of the concurrence of the $2e$ singlet state in more general

cases, and in particular for the *single* elliptic QD of Ref. [7]. This is based on our finding that the concurrence of the singlet state is directly related to the degree of parity breaking present in the unrestricted Hartree-Fock (UHF) orbitals (see below) resulting from our calculations.

We show that knowledge of the dot shape and the $J(B)$ curve allows theoretical determination of the degree of entanglement. This supports the experimental assertion [7] that cotunneling spectroscopy can probe properties of the electronic wave function of the QD, and not merely its low-energy spectrum.

The hamiltonian for two 2D interacting electrons is

$$\mathcal{H} = H(\mathbf{r}_1) + H(\mathbf{r}_2) + e^2/(\kappa r_{12}), \quad (1)$$

where the last term is the Coulomb repulsion, κ is the dielectric constant, and $r_{12} = |\mathbf{r}_1 - \mathbf{r}_2|$. $H(\mathbf{r})$ is the single-particle hamiltonian for an electron in an external perpendicular magnetic field \mathbf{B} and an appropriate confinement potential. For an elliptic QD, the single-particle hamiltonian is written as

$$H(\mathbf{r}) = T + \frac{1}{2}m^*(\omega_x^2 x^2 + \omega_y^2 y^2) + \frac{g^* \mu_B}{\hbar} \mathbf{B} \cdot \mathbf{s}, \quad (2)$$

where $T = (\mathbf{p} - e\mathbf{A}/c)^2/2m^*$, with $\mathbf{A} = 0.5(-By, Bx, 0)$ being the vector potential in the symmetric gauge. m^* is the effective mass and \mathbf{p} is the linear momentum of the electron. The last term in Eq. (2) is the Zeeman interaction with g^* being the effective g factor, μ_B the Bohr magneton, and \mathbf{s} the spin of an individual electron.

Our method for solving the two-body problem defined by the hamiltonian (1) consists of two steps. In the first step, we solve selfconsistently the ensuing unrestricted Hartree-Fock (UHF) equations allowing for breaking of the total spin [and *parity* along the long axis (x -axis) of the elliptic QD]. For the $S_z = 0$ solution, this step produces two single-electron orbitals $u_{L,R}(\mathbf{r})$ that are localized left (L) and right (R) of the center of the QD. At this step, the many-body wave function is a single Slater determinant $\Psi_{\text{UHF}}(1 \uparrow, 2 \downarrow) \equiv |u_L(1 \uparrow)u_R(2 \downarrow)\rangle$ made out of the two occupied UHF spin-orbitals $u_L(1 \uparrow) \equiv$

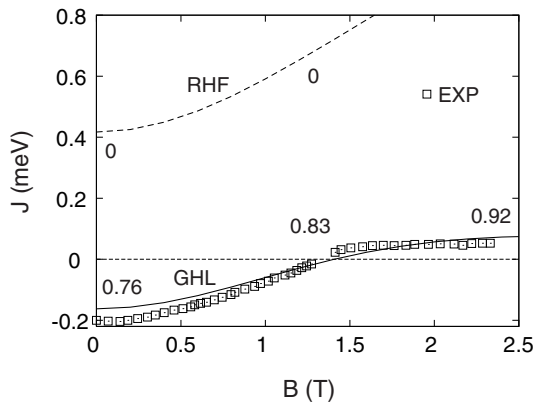


FIG. 1: The singlet-triplet splitting $J = E^s - E^t$ as a function of the magnetic field for an elliptic QD with $\hbar\omega_x = 1.2$ meV and $\hbar\omega_y = 3.3$ meV (these values correspond to the device of Ref. [7]). Lower (solid) curve: The GHL (broken-symmetry UHF + restoration of symmetries) result. Upper (dashed) curve: The restricted HF (RHF, no symmetry breaking) result. The experimental measurements are denoted by the open squares [7]. The material parameters used are: $m^*(\text{GaAs}) = 0.067m_e$, $\kappa = 22.0$, and $g^* = 0$ (see text). The calculated values for the concurrence of the singlet GHL state (C^s , see text) at $B = 0, 1.3$ T, and 2.5 T are also displayed. In the singlet RHF case (upper curve), the concurrence is identically zero for all values of B . Note that our sign convention for J is opposite to that in Ref. [7].

$u_L(\mathbf{r}_1)\alpha(1)$ and $u_R(2\downarrow) \equiv u_R(\mathbf{r}_2)\beta(2)$, where $\alpha(\beta)$ denotes the up (down) [\uparrow (\downarrow)] spin. This UHF determinant is an eigenfunction of the projection S_z of the total spin $\mathbf{S} = \mathbf{s}_1 + \mathbf{s}_2$, but not of \mathbf{S}^2 (or the parity space-reflection operator).

In the second step, we restore the broken parity and total-spin symmetries by applying to the UHF determinant the projection operator [6] $P^{s,t} = 1 \mp \varpi_{12}$, where the operator ϖ_{12} interchanges the spins of the two electrons; the minus sign corresponds to the singlet. The final result is a generalized Heitler-London (GHL) two-electron wave function $\Psi_{\text{GHL}}^{s,t}(\mathbf{r}_1, \mathbf{r}_2)$ for the ground-state singlet (index s) and first-excited triplet (index t), which uses the UHF localized orbitals,

$$\Psi_{\text{GHL}}^{s,t}(\mathbf{r}_1, \mathbf{r}_2) \propto (u_L(\mathbf{r}_1)u_R(\mathbf{r}_2) \pm u_L(\mathbf{r}_2)u_R(\mathbf{r}_1))\chi^{s,t}, \quad (3)$$

where $\chi^{s,t} = (\alpha(1)\beta(2) \mp \alpha(2)\beta(1))$ is the spin function for the $2e$ singlet and triplet states.

The use of *optimized* UHF orbitals in the GHL is suitable for treating *single elongated* QDs. The GHL is equally applicable to double QDs with arbitrary interdot-tunneling coupling [6]. In contrast, the Heitler-London (HL) treatment [10] (known also as Valence bond), where non-optimized “atomic” orbitals of two isolated QDs are used, is appropriate only for the case of a double dot with small interdot-tunneling coupling [3, 11].

Both the GHL singlet, Ψ_{GHL}^s , and the GHL triplet, Ψ_{GHL}^t , cannot be reduced to a single Slater determinant.

They are always the sum of two Slater determinants, i.e., $\Psi_{\text{GHL}}^{s,t} \propto |u_L(1\uparrow)u_R(2\downarrow)\rangle \mp |u_L(1\downarrow)u_R(2\uparrow)\rangle$, and thus they represent states with intrinsic entanglement [3, 6], a property that underlies the operation of the quantum logic gate.

The 2D UHF equations that we are using are described in detail in Ref. [1(c)]. For the formulas which enable calculation of the energies $E_{\text{GHL}}^{s,t}$ for the special case of the two-electron wave function (3), see Refs. [6, 12]. The key point is that we exploit an additional variational freedom by allowing for different orbitals [here $u_L(\mathbf{r})$ and $u_R(\mathbf{r})$] for the two spin directions (up and down). Under appropriate conditions, the UHF equations do indeed have solutions associated with two spatially separated orbitals (symmetry breaking is present). We note, however, that for sufficiently weak Coulomb repulsion (very large dielectric constant κ , see below), the two orbitals $u_L(\mathbf{r})$ and $u_R(\mathbf{r})$ do collapse onto the same single orbital $u(\mathbf{r})$, and there is no symmetry breaking.

Another pertinent point here is that the orbitals $u_{L,R}(\mathbf{r})$ are expanded in a real Cartesian harmonic-oscillator basis, namely,

$$u_{L,R}(\mathbf{r}) = \sum_{j=1}^K C_j^{L,R} \varphi_j(\mathbf{r}), \quad (4)$$

where the index $j \equiv (m, n)$ and $\varphi_j(\mathbf{r}) = X_m(x)Y_n(y)$, with $X_m(Y_n)$ being the eigenfunctions of the one-dimensional oscillator in the $x(y)$ direction with frequency $\omega_x(\omega_y)$. The parity operator \mathcal{P} yields $\mathcal{P}X_m(x) = (-1)^m X_m(x)$, and similarly for $Y_n(y)$. The expansion coefficients $C_j^{L,R}$ are real for $B = 0$ and complex for finite B .

We turn now to the interpretation of the measurements of Ref. [7]. To model the experimental elliptic QD device, we take, following Ref. [7], $\hbar\omega_x = 1.2$ meV and $\hbar\omega_y = 3.3$ meV. The effective mass of the electron is taken as $m^* = 0.067m_e$ (GaAs). Since the experiment did not resolve the lifting of the triplet degeneracy caused by the Zeeman term, we take $g^* = 0$. Using our two step method described above, we calculate the singlet-triplet splitting $J_{\text{GHL}}(B) = E_{\text{GHL}}^s(B) - E_{\text{GHL}}^t(B)$ as a function of the magnetic field in the range $0 \leq B \leq 2.5$ T. Similar to an earlier study [5], we find that a weakening of the Coulomb repulsion from its value in GaAs ($\kappa = 12.9$) is required in order to reproduce the experimental $J(B)$ curve. The effect of screening by the gates can be modeled, to first approximation, by increasing κ [5, 13]. Indeed, with $\kappa = 22.0$, very good agreement with the experimental data (see Fig. 1) is obtained. In particular, we note the singlet-triplet (ST) crossing about 1.3 T, and the backbending of the $J(B)$ curve beyond this crossing.

In Fig. 1, we also plot for $\kappa = 22.0$ the $J_{\text{RHF}}(B)$ curve [upper (dashed) line] obtained from the *restricted* HF (RHF) calculation, namely for a self-consistent Hartree-Fock variation with the restriction that the *parity be*

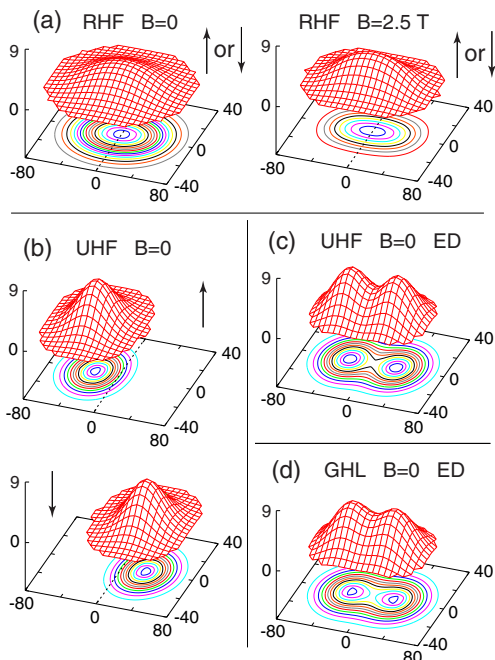


FIG. 2: Spin-up and spin-down orbitals (modulus square) and total electron densities (EDs) associated with the singlet state of two electrons in the elliptic QD. The arrows indicate a spin-up or a spin-down electron. (a) Doubly occupied orbitals of the parity-preserving RHF at $B = 0$ (left) and $B = 2.5$ T (right). (b) Orbitals of the broken-symmetry UHF at $B = 0$. (c-d) EDs at $B = 0$ for the UHF (c) and the GHL (d) wave functions. The GHL ED is larger in the region between the two humps compared to the UHF one; this is indicative of covalent bonding. The rest of the parameters are as in Fig. 1. Lengths in nm and orbital densities in 10^{-4} nm^{-2} .

preserved, so that there is no symmetry breaking and both the spin-up and spin-down electrons occupy the same spatial orbital [i.e., in this approximation $u_L(\mathbf{r}) = u_R(\mathbf{r}) = u(\mathbf{r})$]. The $J_{\text{RHF}}(B)$ curve fails substantially to reproduce the experimental results. The RHF curve disagrees with the experimental trends in two important ways: (I) $J_{\text{RHF}}(0)$ is larger than zero, which not only contradicts the experiment, but also a fundamental theoretical result [1(b), 14] that states that for two electrons at zero magnetic field the singlet is always the ground state, and (II) The $J_{\text{RHF}}(B)$ curve diverges as B increases, unlike the $J_{\text{GHL}}(B)$ curve (as well as the experimental observation) which bends back after the ST crossing and approaches asymptotically the $J = 0$ line.

The sharp contrast in the behavior of the RHF and GHL results further highlights the significance of the latter. Indeed the behavior of the RHF solution reflects the independent-particle-model nature of the RHF orbitals [see Fig. 2(a)], which leads to a preponderance of the exchange contribution, and thus to spontaneous (but erroneous) magnetization of the electron system. On the other hand, the GHL results in Fig. 1 reflect the fact that

symmetry breaking and electron localization [see orbitals in Fig. 2(b)] reduce the Coulomb repulsion to a degree that compensates for the loss of exchange binding (since the localization reduces the orbital overlap). This is portrayed in formation of a Wigner molecule with the aforementioned agreement with the experimental $J(B)$ curve. The total electron density (ED) of the WM resulting from breaking of symmetry [UHF, Fig. 2(c)] and after restoration of parity (and total-spin) symmetry [GHL, Fig. 2(d)] illustrates the electron molecular dimer. We note that the UHF solutions at $B = 0$ exhibit breaking of the parity for values of κ as large as $\kappa = 40.0$, which indicates that the value of $\kappa = 22.0$ in our calculations places the elliptic device of Ref. [7] well within the regime of strong electron correlations.

The asymptotic energetic convergence (beyond the ST point) of the singlet and triplet states, i.e., [$J(B) \rightarrow 0$ as $B \rightarrow \infty$] is a reflection of the dissociation of the $2e$ molecule, since the ground-state energy of two fully spatially separated electrons (zero overlap) does not depend on the total spin. Indeed, orbitals and EDs for finite B values are similar to those in Figs. 2(b-d), but with enhanced localization reflected in diminished overlaps with increasing B .

Both the GHL singlet and triplet wave functions [Eq. (3)] exhibit entanglement by being the sum of two Slater determinants [6, 8]. However, unlike the triplet GHL state which is maximally entangled (see below), the singlet GHL wave function may exhibit a reduced degree of entanglement, as was found from the Hund-Mulliken treatment of the double dot [9]. For purposes of quantum computing, it is necessary to be able to extract from this GHL singlet a quantitative measure of the degree of entanglement, e.g., the corresponding value of the concurrence \mathcal{C} [8, 9]. The concurrence, however, was introduced for the Hilbert space associated with the *bonding* and *antibonding* orbitals of a double dot molecule [8, 9]. In our case of a single elliptic QD, the concept of a bonding and antibonding orbital does not straightforwardly apply. Rather, we need to utilize the universal symmetry properties of the bonding and antibonding orbitals with respect to the parity operator, namely, the bonding orbital is symmetric (+), and the antibonding orbital is antisymmetric (−) with respect to reflection about the origin of the x -axis. We first notice that, due to the symmetry breaking, the UHF orbitals $u_L(\mathbf{r})$ and $u_R(\mathbf{r})$ are not eigenstates of the parity operator, and we proceed to separate the symmetric $\Phi^+(\mathbf{r})$ and antisymmetric $\Phi^-(\mathbf{r})$ components in their expansion given by Eq. (4). That is, we write $u^{L,R}(\mathbf{r}) \propto \Phi^+(\mathbf{r}) \pm \xi \Phi^-(\mathbf{r})$; note that $\Phi^+(\mathbf{r})$ and $\Phi^-(\mathbf{r})$ are eigenfunctions of the parity operator. Subsequently, with the use of Eq. (3), the GHL singlet can be rearranged as follows:

$$\Psi_{\text{GHL}}^s \propto |\Phi^+(1 \uparrow)\Phi^+(2 \downarrow)\rangle - \eta|\Phi^-(1 \uparrow)\Phi^-(2 \downarrow)\rangle, \quad (5)$$

where the coefficient in front of the second determinant,

TABLE I: Left: Expansion coefficients $C_j^{L,R}$ [See Eq. (4)] for the broken-symmetry UHF orbitals $u_L(\mathbf{r})$ and $u_R(\mathbf{r})$ at $B = 0$ and $\kappa = 22.0$. Right: Expansion coefficients for the RHF common orbital $u(\mathbf{r})$. The real-Cartesian-harmonic-oscillator basis functions are given by $\varphi_j(\mathbf{r}) = X_m(x)Y_n(y)$. The running index j stands for the pair (m, n) , where m and n denote the number of nodes along the x and y directions, respectively. A total of $K = 79$ basis states $\varphi_j(\mathbf{r})$ were used. However, only coefficients with absolute value larger than 0.01 are listed here. For numbers with a \pm in the front, the $+$ corresponds to the left (L) orbital and the $-$ to the right (R) one.

UHF		RHF	
$j (m, n)$	$C_j^{L,R}$	$j (m, n)$	C_j
1 (0,0)	0.7990	1 (0,0)	0.9710
2 (1,0)	± 0.5600	3 (2,0)	0.2310
3 (2,0)	0.2150	7 (4,0)	0.0172
5 (3,0)	± 0.0104	10 (0,2)	0.0613
7 (4,0)	-0.0180		
10 (0,2)	0.0253		

$\eta = \xi^2$, is the so-called interaction parameter [9]. Knowing η allows a direct evaluation of the concurrence of the singlet state, since $C^s = 2\eta/(1+\eta^2)$ [9]. Note that $\Phi^+(\mathbf{r})$ and $\Phi^-(\mathbf{r})$ are properly normalized and that they are by construction orthogonal.

For the GHJ triplet, one obtains an expression independent of the interaction parameter η , i.e.,

$$\Psi_{\text{GHJ}}^t \propto |\Phi^+(1 \uparrow)\Phi^-(2 \downarrow)\rangle + |\Phi^+(1 \downarrow)\Phi^-(2 \uparrow)\rangle, \quad (6)$$

which is a maximally ($C^t = 1$) entangled state. Note that underlying the analysis of Ref. [7] is a *conjecture* that wave functions of the form given in Eqs. (5) and (6) describe the two electrons in the elliptic QD.

To make things more concrete, we display in TABLE I for $B = 0$ (and $\kappa = 22.0$) the coefficients $C_j^{L,R}$ [see Eq. (4)] that specify the broken-symmetry UHF orbitals in the real Cartesian harmonic-oscillator basis. Indeed, we find that there are contributions from both symmetric and antisymmetric basis functions $X_m(x)Y_n(y)$ along the x -axis, since both even and odd m indices are present. The n indices are all even, since there is no symmetry breaking along the y -axis. Naturally, all the m indices in the expansion of the RHF common $u(\mathbf{r})$ orbital are even, since in this case the parity is preserved. One can immediately check that $\xi = \left(\sum_{j (m \text{ odd})}^K |C_j^L|^2 / \sum_{j (m \text{ even})}^K |C_j^L|^2\right)^{1/2}$.

For the RHF singlet $\xi = 0$, since there no coefficients with odd m indices (TABLE I). For the GHJ singlet, we calculate the interaction parameter $\eta = \xi^2$ and the concurrence C^s for the device of Ref. [7] in the magnetic-field range $0 \leq B \leq 2.5$ T. We find that starting with $\eta = 0.46$ ($C^s = 0.76$) at $B = 0$, the interaction parameter (singlet-state concurrence) increases monotonically to $\eta = 0.65$ ($C^s = 0.92$) at $B = 2.5$ T. At the intermediate value corresponding to the ST transition ($B = 1.3$

T), we find $\eta = 0.54$ ($C^s = 0.83$). Our $B = 0$ theoretical result for η and C^s are in remarkable agreement with the experimental estimates [7] of $\eta = 0.5 \pm 0.1$ and $C^s = 0.8$, which were based solely on conductance measurements below the ST transition (i.e., near $B = 0$). Our theoretical values for the singlet-state concurrence are marked on the GHJ curve in Fig. 1. We also display in this figure the value of C^s for the RHF single-determinant solution (upper curve). The RHF value for this quantity (and also for η) vanishes identically for all B values. Thus the shape (and values) of the experimental $J(B)$ curve portray directly the degree of electron localization and the entanglement associated with the singlet state in Eq. (3). Note that our calculated results are based on the energetics of the singlet-triplet splitting alone, and thus they provide a reliable and independent alternative method for extracting the degree of singlet-state entanglement for all values of B .

In conclusion, we have shown formation of an electron molecular dimer in an elliptic QD (Fig. 2) for screened interelectron repulsion characterized by a singlet-triplet splitting $J(B)$ that agrees with experiment (Fig. 1). Furthermore we showed that, from a knowledge of the dot shape and of $J(B)$, theoretical analysis along the lines introduced here allows probing of the correlated ground-state wave function and determination of its degree of entanglement. Such information is of great value for the implementation of solid-state quantum logic gates. It is also of interest to quantum information theory in general [15, 16]. The present theoretical method and analysis can be straightforwardly extended to double dots with arbitrary interdot-tunneling coupling.

This research is supported by the US D.O.E. (Grant No. FG05-86ER45234), and NSF (Grant No. DMR0205328). We thank M. Pustilnik for comments on the manuscript.

-
- [1] (a) C. Yannouleas and U. Landman, Phys. Rev. Lett. **82**, 5325 (1999); **85**, E2220 (2000); (b) Phys. Rev. B **61**, 15895 (2000); (c) Phys. Rev. B **68**, 035325 (2003).
 - [2] C. Yannouleas and U. Landman, Phys. Rev. Lett. **85**, 1726 (2000); S.A. Mikhailov and N. A. Savostianova, Phys. Rev. B **66**, 033307 (2002).
 - [3] G. Burkard, D. Loss, and D.P. DiVincenzo, Phys. Rev. B **59**, 2070 (1999).
 - [4] S. Tarucha, D.G. Austing, Y. Tokura, W.G. van der Wiel, and L.P. Kouwenhoven, Phys. Rev. Lett. **84**, 2485 (2000).
 - [5] J. Kyriakidis, M. Pioro-Ladriere, M. Ciorga, A.S. Sachrajda, and P. Hawrylak, Phys. Rev. B **66**, 035320 (2002).
 - [6] C. Yannouleas and U. Landman, Int. J. Quantum Chem. **90**, 699 (2002); Eur. Phys. J. D **16**, 373 (2001).
 - [7] D.M. Zumbühl, C.M. Marcus, M.P. Hanson, and A.C. Gossard, Phys. Rev. Lett. **93**, 256801 (2004).
 - [8] J. Schliemann, D. Loss, and A.H. MacDonald, Phys. Rev. B **63**, 085311 (2001).

- [9] V.N. Golovach and D. Loss, Phys. Rev. B **69**, 245327 (2004).
- [10] H. Heitler and F. London, Z. Phys. **44**, 455 (1927).
- [11] An immediate extension of the simple HL method known as the Hund-Mulliken method is also restricted to the case of a double QD with weak interdot tunneling.
- [12] C. Yannouleas and U. Landman, J. Phys.: Condens. Matter **14**, L591 (2002).
- [13] Unlike the strongly elliptical case of Ref. [7], Ref. [5] measured the $J(B)$ curve *before* the singlet-triplet splitting for a $2e$ lateral GaAs dot with a shape only slightly deformed away from the circular. No estimates for the degree of entanglement were reported.
- [14] D.C. Mattis, *The Theory of Magnetism*, Springer Series in Solid-State Sciences No. 17 (Springer, New York, 1988), Vol. I, Sec. 4.5.
- [15] F. Verstraete, M.A. Martin-Delgado, and J.I. Cirac, Phys. Rev. Lett. **92**, 087201 (2004).
- [16] H. Fan, V. Korepin, and V. Roychowdhury, Phys. Rev. Lett. **93**, 227203 (2004).